The Seybold Report

ISSN 1533-9211

DOI: 10.5281/zenodo.8311139

A COMPARABLE PERFORMANCE BY IMPLEMENTING A TWO AND THREE PERIOD STAGGERED FOR OPTIMIZING THE DEEPEST MINIMUM AT A FREQUENCY RESPONSE

MOHAMMED JASIM AL- SUMAIDAEE *

B.D.S, M.Sc. Communication Engineering, Ph.D. Student, Department of ECE, KL University, India.
*Corresponding Author Email: mgm1947@yahoo.com

M. SIVA GANGA PRASAD

B.D.S., M.Sc., Ph.D. Antenna and Wireless Communication, Professor, Department of ECE, KL University, India.

DHAHIR ABDULHADE ABDULAH

B.D.S., M.Sc., Ph.D. Computer Science, Professor, Department of computer, College of Science, University of Diyala.

Abstract

By varying the intervals between pulses or staggering them, we can increase the blind speeds. Blind speeds attained with a constant PRF are lost because to the scattered PRFs. This study implements a two- and three-period staggered frequency response to improve the deepest or minimum value in the velocity region and achieve equivalent performance.

Keywords: Two period staggers, Three Period Staggers, Deepest Minimum Frequency, Moving Target Indication (MTI)

INTRODUCTION

By reducing the return from stationary clutter return, moving target indication (MTI) filters increase the probability of detecting moving targets. Single line cancellers, the simplest and most well-known type of MTI filter, work by subtracting the received signal owing to two successive pulses to cancel the clutter. Using a constant pulse repetition interval (PRI) creates a blind speed problem, which is a significant drawback of MTI filtering. Changing the intervals between pulses can help eliminate the blind speed and frequency response nulls. Interpulse period are optimized by numerical methods. Combining analytical filter optimization with numerical interpulse period optimization, a new technique has been devised. The improvement in the power ratio of signals -to-clutter as a function of frequency can be useful. We'll call this improvement in the signal-to-clutter ratio. It's closely related to improvement factor.

Staggered MTI PRF

However, the fact that the pulse spacing is uniform facilitates simplification of a number of mathematical expressions defining performance, making the unstaggered PRF (MTI) a particular case of staggered PRF for which the pulse spacing is constant. While conventional processors still exhibit blind speed, this simplification allows for the invention of new classes of processors for the unstaggered PRF system and greatly simplifies the mathematical design

The Seybold Report
ISSN 1533-9211
DOI: 10.5281/zenodo.8311139

techniques for others. This is a feature of any PRF system that does not use frequency hopping. Doppler frequencies above the system PRF might be necessary if the radar system's needs are particularly demanding.

There needs to be a way to lessen or do away with these arbitrary speeds. Frequency agility and the staggered PRF are two ways to lower these blind speeds.

The increased blind speed is the only one that can be overcome by frequency agility. To solve the blind speed issue in an MTI radar system, staggered pulse repetition intervals are commonly used.

Effect of two and three period staggering upon frequency response Coherent MTI radar works via phase comparison of all echoes to see if they are coherent with a reference phase. In the event of a reflection from a moving object, the subtractor will produce an output.

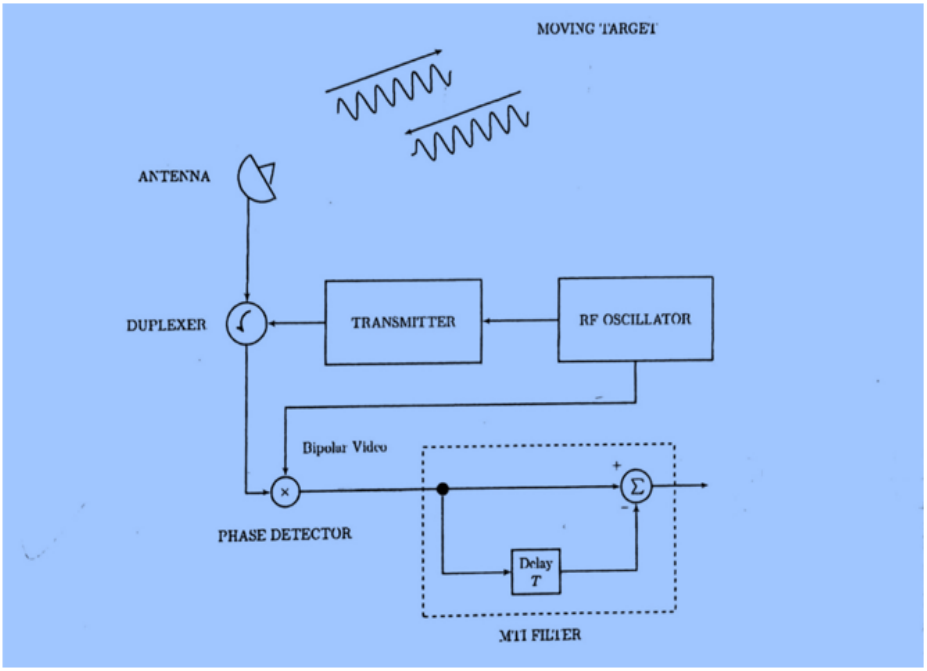

Figure 1: Simplified Block Diagram of a Coherent MTI System

"For uniform PRF a Doppler frequency associated with a target speed (V) and wave length (λ) is ($\frac{2v}{\lambda}$)"

Pulse trains modulated by a sinusoidal envelope are the coherent detector's output.

$$E = \sin 2\pi fdt \quad \text{.....} \quad (1)$$

The amplitude of pulses in a uniform (non-staggered) PRF is calculated by sampling the envelope at specific moments.

$$tn = To + nT \quad \text{.....} \quad (2)$$

The Seybold Report
ISSN 1533-9211
DOI: 10.5281/zenodo.8311139

The system's reaction is the mean of the responses to individual Pulse trains of period (T- δ)/ (T+ δ) at main delay line length T and stagger delay (δ).

The system responds as two Pulse separations because the first canceller subtracts Pulse pairs separated by (T+δ) and (T- δ) and feeds the difference into the second canceller.

To achieve a wide variety of pulse spacing with just a modest increase in complexity of equipment, a three-period Stagger system switches the delay line, T, δto give the periods (T + δ), T, (T- δ).

The amplitude of nth-sample:

$$\mathbf{An= \sin 2\pi.fd\ (to+nT)} \quad \ldots\ldots\ldots\ldots\ldots\ldots \quad \mathbf{(3)}$$

The envelope is sampled at times:

to + nT for n even

and

to + nT + δ for n odd

therefore

$$\mathbf{tn = to + \frac{\delta}{2} + nT + (-1)^n \frac{\delta}{2}} \quad \mathbf{for\ all\ n} \ \ldots\ldots\ldots\ldots\ldots \quad \mathbf{(4)}$$

In case of two period stagger, the amplitude of nth pulses is:

$$\mathbf{An= \sin 2\pi.fd\ (to + \frac{\delta}{2} + nT + (-1)^n \frac{\delta}{2})} \ \ldots\ldots\ldots\ldots\ldots\mathbf{(5)}$$

By putting

$$\mathbf{t1 = to + \frac{\delta}{2}} \ \ldots\ldots\ldots\ldots\ldots\ldots\ldots\ldots \quad \mathbf{(6)}$$

Expanding the expression:

$$\mathbf{An= \sin 2\,\pi\, fd\ (t1+nT) \cos 2\,\pi\, fd\ (-1)^n \frac{\delta}{2}}$$

$$\mathbf{+ \cos 2\,\pi\, fd(t1 + nT).\ sin2\,\pi\, fd(-1)\ n\ \frac{\delta}{2}} \ \ldots\ldots\ldots\ldots \quad \mathbf{(7)}$$

for n integer $(-1)^2 = \cos n\,\pi$

$$\mathbf{An = \sin 2\,\pi\, fd\ (t1+nT) \cos 2\,\pi\, fd\ \frac{\delta}{2} + \cos 2\,\pi\, fd\ (t1+nT) \cos \pi\ n \sin 2\,\pi\, fd\ \frac{\delta}{2}} \ldots\ldots \quad \mathbf{(8)}$$

$$\therefore \text{An} = \sin 2\,\pi\, fd\ (t1+nT) \cos 2\,\pi\, fd\ \frac{\delta}{2} + \frac{1}{2} \cos 2\,\pi\, fd\ [(t1+n(T+ \frac{1}{2fd})] \sin 2\,\pi\, fd\ \frac{\delta}{2}$$

$$\mathbf{+\ \frac{1}{2} \cos 2\,\pi\, fd\ (t1+n(T - \frac{1}{2fd})\ )\ \sin 2\,\pi\, fd\ \frac{\delta}{2}} \ \ldots\ldots\ldots\ldots\ldots\ldots\ldots\ldots \quad \mathbf{(9)}$$

Put:

$$\cos 2\,\pi\, fd[(t1+nT\ (1+\frac{1}{2Tfd})] \equiv \cos 2\,\pi\, f_1\ (t1+nt)$$

The Seybold Report
ISSN 1533-9211
DOI: 10.5281/zenodo.8311139

and

fd [(t1 + nT (1 + $\frac{1}{2Tfd}$)] ≡ f1 (t1+nT)

fdt1 = f1t1\`

and

fdnT (1 + $\frac{1}{2Tfd}$) = f1nT

∴ f1 = fd + (1 + $\frac{1}{2Tfd}$)

∴ fr = $\frac{1}{T}$

∴ f1 = fd + $\frac{1}{2T}$

f1 = fd + $\frac{1}{2}$ fr

similarly:

f2 = fd - $\frac{1}{2}$ fr

finally:

$$\mathbf{An = \sin 2\pi\, fd\, (t1+nT) \cos\ \pi\, fd\, \delta + \cos 2\pi\, (fd + \tfrac{1}{2} fr)\, (t1+nT)\, \tfrac{1}{2} \sin \pi\, fd\, \delta + \cos 2\pi\, (fd - \tfrac{1}{2} fr)\, (t1+nT)\, \tfrac{1}{2} \sin \pi\, fd\, \delta} \quad \text{.......................................} \quad \mathbf{(10)}$$

Where:

An: amplitude of nth pulses

To: total time of pulse

δ : stagger delay

T : period time

The frequency response G(fd) of the canceller is periodic in fr

So that:

$$\mathbf{G\, (fd + \tfrac{1}{2} fr) = G\, (fd - \tfrac{1}{2} fr)} \quad \text{...} \quad \mathbf{(11)}$$

And the two side band responses can be added together:

The r.m.s output of the canceller is thus:

$$\mathbf{(Vout)^2 = [G^2\, (fd) \cos^2 \pi\, fd\, \delta + G^2\, (fd + \tfrac{1}{2} fr) \sin \pi\, fd\, \delta]} \quad \text{..................} \quad \mathbf{(12)}$$

for double cancellation:

ISSN 1533-9211

DOI: 10.5281/zenodo.8311139

$G(fd) = \sin^2 \pi fdT$

And r.m.s cancelled output will be:

$$(Vout)^2 = \sin^4 \pi fdT \cos^2 \pi fd\,\delta + \cos^4 \pi fdT \sin^2 \pi fd\,\delta \ldots\ldots\ldots\ldots (13)$$

In case of three period stagger successive period

$T - \delta, T, T + \delta$

The amplitude nth pulses will be?

$$An = \sin 2\pi fd\,[to + nT + \frac{\delta}{2}\{1 + (\frac{3}{4}\cos\frac{2n\pi}{3} - \frac{1}{3})\}] \ldots\ldots\ldots\ldots\ldots (14)$$

Suppose

$t1 = to + \frac{\delta}{2}$

$$An = \sin 2\pi fd\{(t1 + nT) + \frac{1}{2}(\frac{4}{3}\cos\frac{2n\pi}{3} - \frac{1}{3})\,\delta\} \ldots\ldots\ldots\ldots\ldots\ldots (15)$$

Expanding the expression will be :

$$An = \sin 2\pi fd\,(t1 + nT)\cos\pi fd\,(\frac{4}{3}\cos\frac{2n\pi}{3} - \frac{1}{3})\,\delta$$

$$+ \cos 2\pi fd\,(t1+nT)\sin\pi fd\,(\frac{4}{3}\cos\frac{2n\pi}{3} - \frac{1}{3})\,\delta \ldots\ldots\ldots\ldots\ldots\ldots (16)$$

Therefore:

$$An = 2\pi fd\,(t1 + nT)\cos\pi fd\,\delta - \frac{1}{3}\cos 2\pi fd\,(t1 + nT)\sin\pi fd\,\delta$$

$$+ \frac{4}{3}[\frac{1}{2}\{\cos(2\pi fd\,(t1 + nT) + \frac{2n\pi}{3}) + \cos(2\pi fd\,(t1 + nT) - \frac{2n\pi}{3})\}] ..(17)$$

Suppose:

$\cos(2\pi fd\,(t1 + nT) + \frac{2n\pi}{3})$

$\cos 2\pi fd\,(t1 + nT + \frac{2}{3fd})$

$\cos 2\pi fd\,(t1 + nT + \frac{2}{3fd}) \equiv \cos 2\pi f1\,(t1 + nT)$

$fd\,[t1 + nT(1 + \frac{1}{3Tfd})] \equiv f1\,(t1 + nT)$

$fd\,t1 = f1\,t1$

$fd\,nT(1 + \frac{1}{3Tfd}) = f1\,nT$

$fd(1 + \frac{fr}{3fd}) = f1$

$f1 = fd + \frac{fr}{3}$

DOI: 10.5281/zenodo.8311139

$$An = \sin 2\pi fd\,(t1 + nT) \cos \pi fd\,\delta - \frac{1}{3} \cos 2\pi fd\,(t1 + nT) \sin \pi fd\,\delta$$

$$+ \frac{2}{3} \cos 2\pi\,(fd + \frac{fr}{3})\,(t1 + nT) \sin \pi fd\,\delta + \frac{2}{3} \cos 2\pi\,(fd - \frac{fr}{3})\,(t_1 + nT) \sin \pi fd\,\delta \ldots\ldots (18)$$

The r.m.s canceller output for three period staggers:

$$(Vout)^2 = [G^2(fd)\,(\cos^2 \pi fd\,\delta + \frac{1}{9} \sin^2 \pi fd\,\delta) + G^2(fd + \frac{fr}{3})\,\frac{4}{9}\,\sin^2 \pi fd\,\delta$$

$$+ G^2(fd - \frac{fr}{3})\,\frac{4}{3}\,\sin^2 \pi fd\,\delta] \ \ldots\ldots (19)$$

for double cancellation

$G(fd) = \sin^2 \pi\, fdT$

The r.m.s canceller output will be:

$$(Vout)^2 = \sin^4 \pi fdT\,(\cos^2 \pi fd\,\delta + \frac{1}{9} \sin^2 \pi fd\,\delta) + \sin^4(\pi fdT + \frac{\pi}{3})\,\frac{4}{9} \sin^2 \pi fd\,\delta + \sin^4(\pi fdT - \frac{\pi}{3})\,\frac{4}{9} \sin^2 \pi fd\,\delta \ \ldots\ldots (20)$$

The two next expressions represent the response of MTI system to targets at different speeds

The expressions can compute and plotted as function of the angle (π fdT) for a given values of (δ, T).

For two period staggers with cancellation the r.m.s cancelled output is:

$$|Hs(v)|^2 = \sin^4 \pi fdT \cos^2 \pi fd\,\delta + \cos^4 \pi fdT \sin^2 \pi fd\,\delta \ \ldots\ldots (21)$$

and for three period staggers with double cancellation

The r.m.s cancelled output is:

$$|Hs(v)|^2 = \sin^4 \pi fdT - \frac{4}{3} \sin^2 \pi fd\ .\ \sin^4 \pi fdT + \frac{1}{2} \sin^2 \pi fd\,\delta \ \ldots\ldots (22)$$

Blind speed limitation

When the argument (πfd T) in the amplitude factor of is (0, π,2π, ---ets), or when; the response of the single delay-line canceller is zero.

$fd = \frac{n}{T} = nfp$

where nfp = 0,1,2, ….

And

fp = "Pulse repetition frequency".

When the d.c component introduced by clutter (n=0) is cancelled out by a delay line canceller, any moving targets whose doppler frequency is also PRF or a multiple thereof are also rejected.

The Seybold Report
ISSN 1533-9211
DOI: 10.5281/zenodo.8311139

The formula for blind speeds, which are those in relation to the target that elicit no MTI response, is as follows.

$Vn = n\lambda /2T = n\lambda fp/2$

n = 1,2,3, ….

Limitations on pulses not generated by continuous-wave (CW) radar are represented by (n), where n is the blind speed. Since pulse radar measures doppler using sampled pulses at the PRF, this issue is inherent to the method.

In order for the first blind speed to be greater than the maximum increase radial velocity from the target, the product (IF) must be large. This necessitates either a very high pulse repetition and frequency or a very long wavelength for the MTI radar.

Other limitation to MTI performance

The effectiveness of MTI radar has its limits. As a result of the following factors, MTI radar performance degrades:

A) Antenna Scanning Modulation

Time taken by the Pulse radar scan antenna to process an Echo signal from a target or clutter, scatterer.

$$\frac{Nb}{fp} = \frac{\theta b}{\theta s} \quad \text{..... (23)}$$

Nb : “Number of pulses received”

fp: “pulse repetition frequency”

θb: “antenna beam width rate in degree”

θs: “antenna scanning rate in degree / second”

The beam width of the frequency spectrum is inversely proportional to the square of the time if the Clutter scatterer is perfectly stationary and there are no instabilities in the equipment.

These limits are sometimes referred to as "antenna scanning modulation," although in reality they are the result of a lack of time. Spending more time honing in on the target will reduce the wide range of distractions.

B) Internal Fluctuation of Clutter

Echoes are usually stationary in nature when striking inanimate things in nature (mountains, rocks, buildings, hills, water towers, fences, thick free cars, etc.). However, there could be a wide variety of other things at play that generate annoying echoes. You can count the echoes of the sea, the rain, the chaff, the big plants, the swaying buildings, etc. As the amplitude and phase of wind-blowing structures shift, so do the clutter echoes, limiting the usefulness of MTI radar.

The Seybold Report
ISSN 1533-9211
DOI: 10.5281/zenodo.8311139

C) Equipment instabilities.

The improvement factor of MTI radar is constrained by the presence of uncancelled clutter echoes brought about by variations in the amplitude, frequency, or phase of the stalo oscillators, the pulse-to-pulse characteristics of the transmitted signal, or errors in timing.

D) Limiting

It is not uncommon for the MTI receiver's limiter to be used to bring the level of interference down to that of the level receiver noise.

MTI radar's hard limiters significantly degrade the system's performance. A limiter equivalent to the MTI radar improvement factor should be imposed on the receiver noise instead.

MTI Improvement Factor

Two metrics typically employed to characterize MTI system performance are presented below. Clutter attenuation (CA) and the MTI improvement factor are two such measures.

To calculate the (CA), divide the clutter power (CI) at the input of the MTI filter by the clutter power (CO) at the output of the filter.

$$\mathbf{CA}=\frac{\mathbf{Ci}}{\mathbf{Co}} \quad \ldots\ldots\ldots\ldots\ldots\ldots\ldots\ldots\ldots\ldots\ldots\ldots\ldots\ldots\ldots\ldots\ldots\ldots \mathbf{(24)}$$

The MTI improvement factor is defined as the ratio of the signal to clutter (SCR) at the output to the (SCR) at the input

$$\mathbf{I} = (\frac{\mathbf{So}}{\mathbf{Co}}) / (\frac{\mathbf{Si}}{\mathbf{Ci}}) \quad \ldots\ldots\ldots\ldots\ldots\ldots\ldots\ldots\ldots\ldots\ldots\ldots\ldots\ldots\ldots\ldots\ldots\ldots \mathbf{(25)}$$

which can be rewritten as:

$$\mathbf{I} = \frac{\mathbf{So}}{\mathbf{Si}} \mathbf{.\ CA} \quad \ldots\ldots\ldots\ldots\ldots\ldots\ldots\ldots\ldots\ldots\ldots\ldots\ldots\ldots\ldots\ldots\ldots\ldots \mathbf{(26)}$$

The ratio so/si is the average power gain of the MTI filter and it's equal to $|H(w)|^2$

from the definition of the improvement factor above

$$\mathbf{I} = \mathbf{G}\frac{\mathbf{Ci}}{\mathbf{Co}} \quad \textbf{where} \quad \mathbf{G} = \frac{\mathbf{So}}{\mathbf{Si}} \quad \ldots\ldots\ldots\ldots\ldots\ldots\ldots\ldots\ldots\ldots\ldots\ldots\ldots\ldots\ldots\ldots \mathbf{(27)}$$

and (Ci) is the clutter at the input of MTI filter and equal

$$\mathbf{Ci} = \int_{\mathbf{O}}^{\infty} \frac{-f^2}{e^{2\delta 2}}\,\mathbf{df} \quad \ldots\ldots\ldots\ldots\ldots\ldots\ldots\ldots\ldots\ldots\ldots\ldots\ldots\ldots\ldots\ldots\ldots\ldots \mathbf{(28)}$$

and (Co) is the clutter residue at the output of MTI filter which equal

$$\mathbf{Co}= \int_{\mathbf{O}}^{\infty} |\mathbf{H(f)}|^2 \ \frac{-f^2}{e^{2\delta 2}}\ \boldsymbol{df} \quad \ldots\ldots\ldots\ldots\ldots\ldots\ldots\ldots\ldots\ldots\ldots\ldots\ldots\ldots\ldots\ldots\ldots\ldots \mathbf{(29)}$$

ISSN 1533-9211

DOI: 10.5281/zenodo.8311139

by applying the definition of average gain to get:

$$\mathbf{G = \frac{T}{N} \int_{O}^{NIT} (\sin^4 af - \frac{4}{3} \sin^2 bf \sin^4 af + \frac{1}{2} \sin^2 bf)\, df \ldots\ldots (30)}$$

Where

a = π T

b = π T $\frac{M}{N}$

where

M = stagger delay

N = canceller delay (main delay)

By applying the definition of improvement factor

$$\mathbf{I = 3. \frac{\frac{1}{2}\sqrt{2\pi}\,\delta}{\frac{1}{2}\sqrt{2\pi}\,\delta\,[\frac{1}{3}e^{-8(\pi T\delta)^2} - \frac{4}{3}e^{-2(\pi T\delta)^2} + 3 + \frac{2}{3}e^{-2(\pi T\delta)^{2\,(4+\frac{M}{N})}}}}$$

$$\mathbf{\frac{}{\text{Cos h } 8\,(\pi T\delta)^2 \frac{M}{N} - \frac{8}{3}e^{-2(\pi T\delta)^{2\,(1+\frac{M^2}{N^2})}} \text{Cos h} 4\,(\pi T\delta)^2 \frac{M}{N}]} \ldots\ldots\ldots\ldots\ldots\ldots\ldots\ldots\ldots (31)}$$

Therefore:

$$I = \frac{1}{1 + \frac{1}{9}e^{-8(\pi T\delta)^2} - \frac{4}{9}e^{-2(\pi T\delta)^2} + \frac{2}{9}e^{-2(\pi T\delta)^{2(4+\frac{M^2}{N^2})}} \cosh 8\,(\pi T\delta)^2 \frac{M}{N}}$$

$$\frac{}{- \frac{8}{9}e^{-2(\pi T\delta)^2 \quad (1+\frac{M^2}{N^2})} \cos h\, 4\,(\pi T\delta)^2 \frac{M}{N}}$$

Finally

$$\mathbf{I = \frac{1}{1 + \frac{1}{3}e^{-8(\pi T\delta)^2} - \frac{4}{3}e^{-2(\pi T\delta)^{2(1+\frac{M^2}{N^2})}} \cos 4(\pi T\delta)^2 \frac{M}{N}} \ldots\ldots\ldots\ldots\ldots\ldots\ldots\ldots\ldots\ldots\ldots (32)}$$

The Seybold Report
ISSN 1533-9211
DOI: 10.5281/zenodo.8311139

Table 1: Deepest Minimum for Two and Three Period Staggers

Two period staggers			Three period staggers		
Frequency response |Hs(v)| (dB)			Frequency response |Hs(v)| (dB)		
Stagger Delay (M)	Main delay line (N)	Deepest Minimum (dB)	Stagger Delay (M)	Main delay line (N)	Deepest Minimum (dB)
5	4	-12	5	1	-50
				3	
10	2	-50	10	2	-50
	3.5			4	
	5			5	
	6.5			6	
	8			8	
15	1.5	-50	15	1	-50
	5			3	
	10			5	
	11.7			9	
				10	
				12	
				13	
25	5	-50	25	1	-50
	10			3	
	15			5	
	20			7	
				9	
				10	
				11	
				13	
				15	
				17	
				19	
				20	
				21	
				23	

Table 2: Frequency Response at Two Period Staggers (Deepest Minimum)

Delay Stagger (M)	Main delay line (N)	$\frac{V}{Vbs}$	Deepest minimum |Hs(V)|(dB)
1	5	0.5	-50
1	10	0.45	-18
		0.51	-18
1	15	0.5	-50
1	20	0.48	-22
		0.52	
1	25	0.5	-50
1	30	0.48	-25
		0.52	

ISSN 1533-9211

DOI: 10.5281/zenodo.8311139

Table 3: Frequency Response at Three Period Staggers (Deepest Minimum)

Delay Stagger (M)	Main delay line (N)	$\frac{V}{Vbs}$	Deepest minimum |Hs(V)|(dB)
1	5	0.18 0.82	-8
1	10	0.1 0.9	-14
1	15	0.08 0.95	-17
1	20	0.05 0.97	-19
1	25	0.04 0.98	-22
1	30	0.03 0.97	-23

CONCLUSION

Staggered blind speeds of MTI radar can be eliminated to a large part by PRF optimization, and the depth of minimum value in the velocity area in the frequency response (|Hs(f)|)2 or improvement factor can be optimized with suitable selection of stagger delay (M). When comparing the minimum gain in signal-to-clutter ratio (SCR) and improvement factor, several relative Optima exhibit large discrepancies. Small values of time on target and of radar Frequency with respect to the improvements factor are favoured. Among the local optima, some good alternatives can be found that combine high improvements factor and high minimum SCR gain

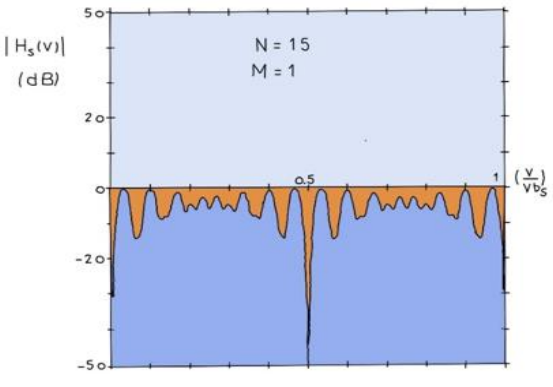

Figure 2: Velocity Response at Stagger Ratio 14:16

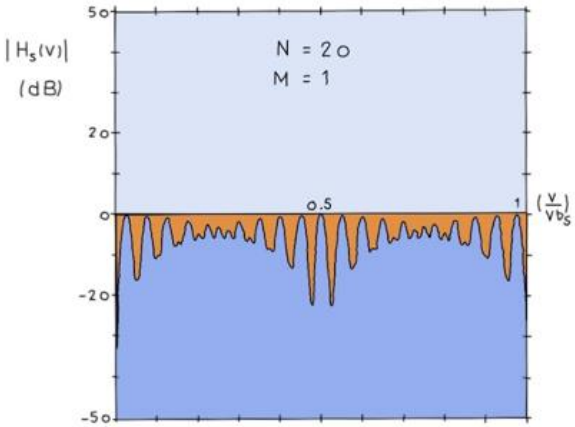

Figure 3: Velocity Response at Stagger Ratio 19:21

ISSN 1533-9211

DOI: 10.5281/zenodo.8311139

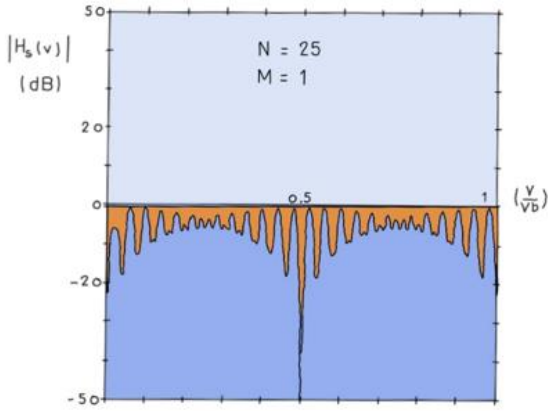

Figure 4: Velocity Response at Stagger Ratio 29:31

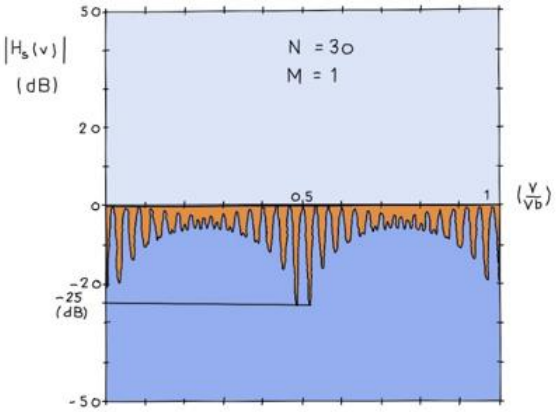

Figure 5: Velocity Response at Stagger Ratio 24:26

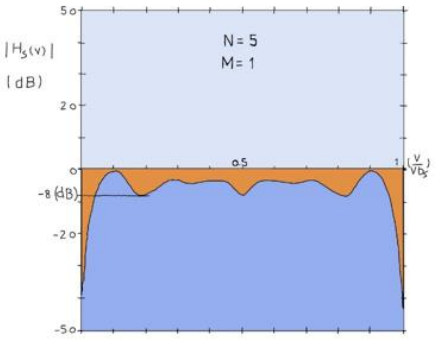

Figure 6: Velocity Response at Stagger Ratio 4:5:6

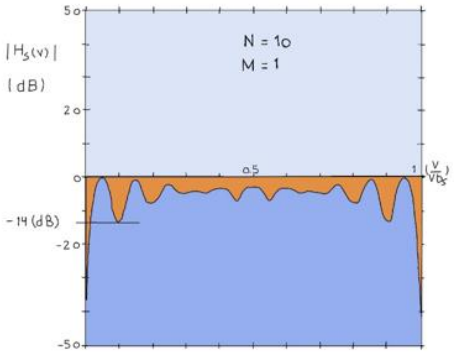

Figure 7: Velocity Response at Stagger Ratio 9:10:11

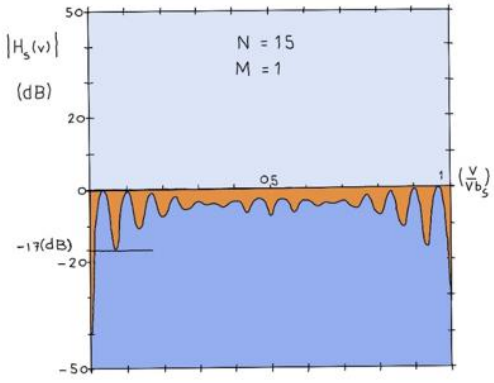

Figure 8: Velocity Response at Stagger Ratio 14:15:16

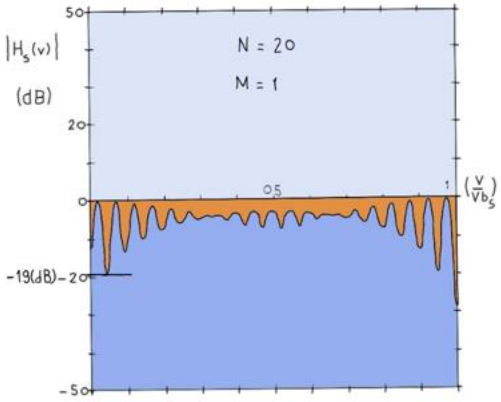

Figure 9: Velocity Response at Stagger Ratio 19:20:21

ISSN 1533-9211

DOI: 10.5281/zenodo.8311139

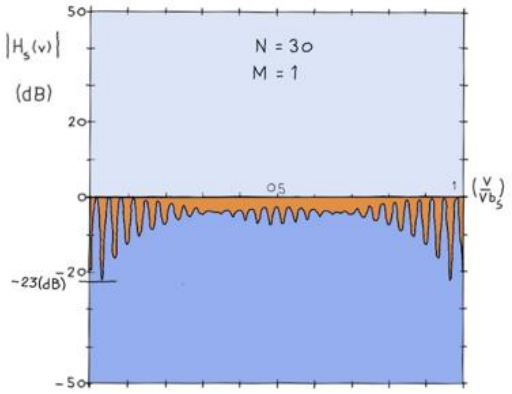

Figure 10: Velocity Response at Stagger Ratio 29:30:31

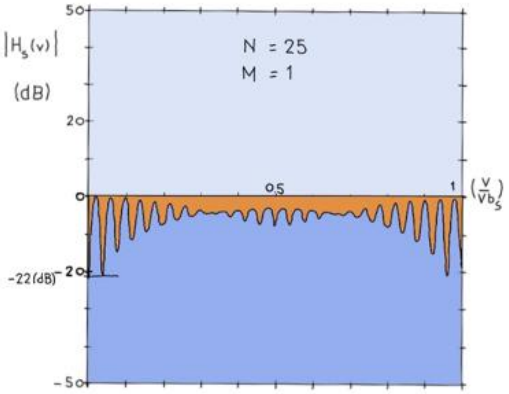

Figure 11: Velocity Response at Stagger Ratio 24:25:26

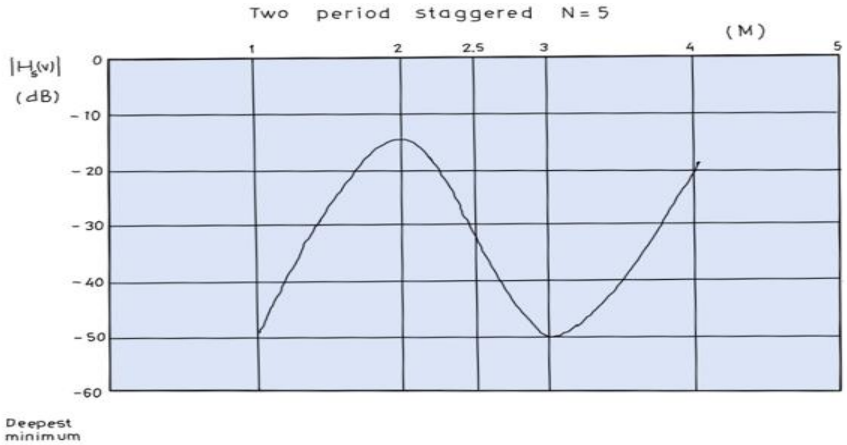

Figure 12: A Deepest Minimum In Response Curve Vs Stagger Delay (M)

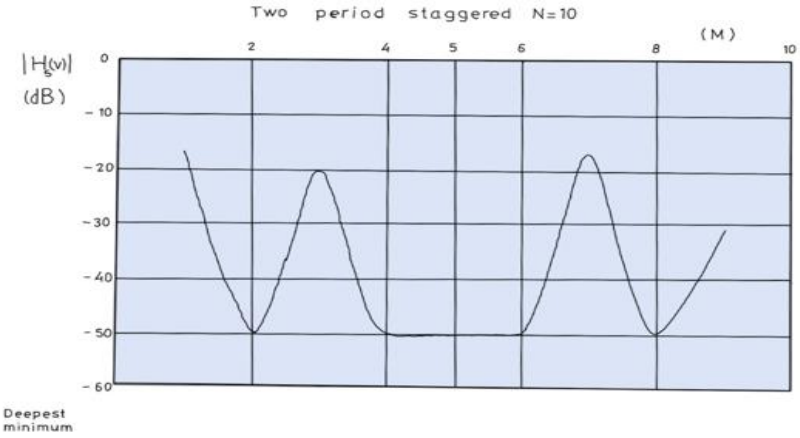

ISSN 1533-9211

DOI: 10.5281/zenodo.8311139

Figure 13: A deepest Minimum in Response Curve Vs Stagger Delay (M)

Figure 14: A Deepest Minimum in Response Curve Vs Stagger Delay (M)

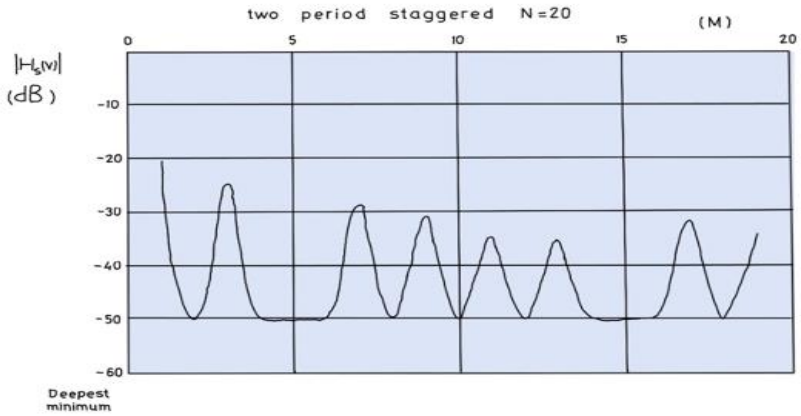

Figure 15: A Deepest Minimum in Response Curve Vs Stagger Delay (M)

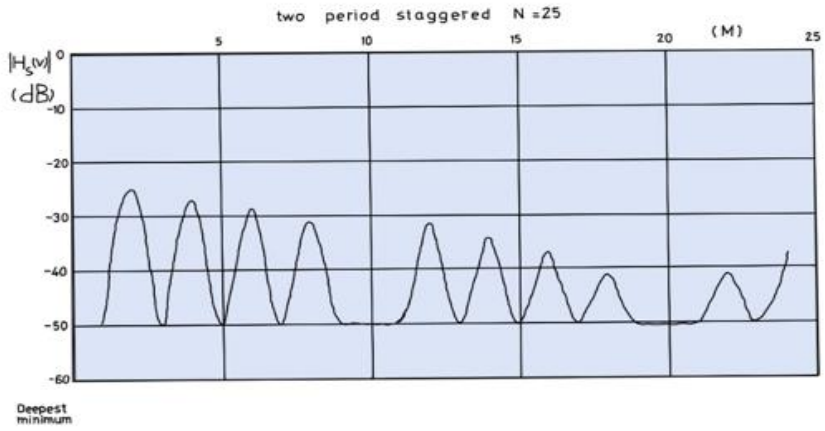

Figure 16: A deepest Minimum in Response Curve Vs Stagger Delay (M)

ISSN 1533-9211

DOI: 10.5281/zenodo.8311139

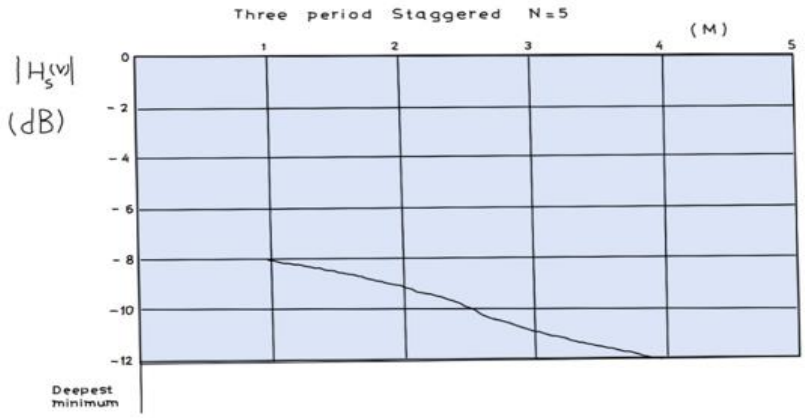

Figure 17: A Deepest Minimum in Response Curve Vs Stagger Delay (M)

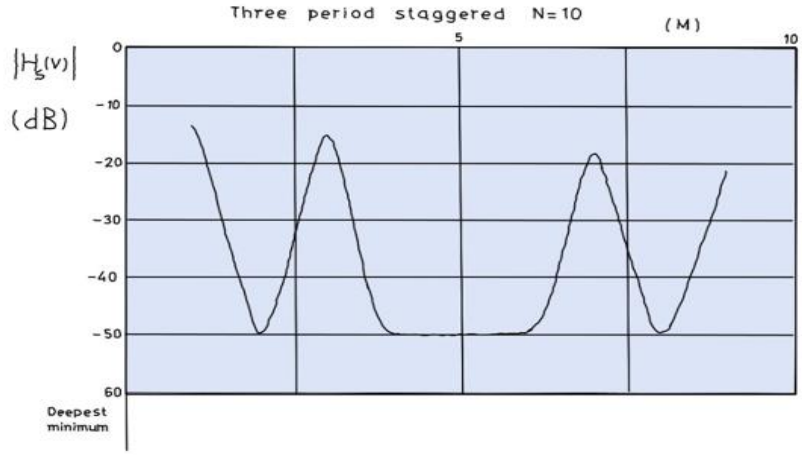

Figure 18: A Deepest Minimum in Response Curve Vs Stagger Delay (M)

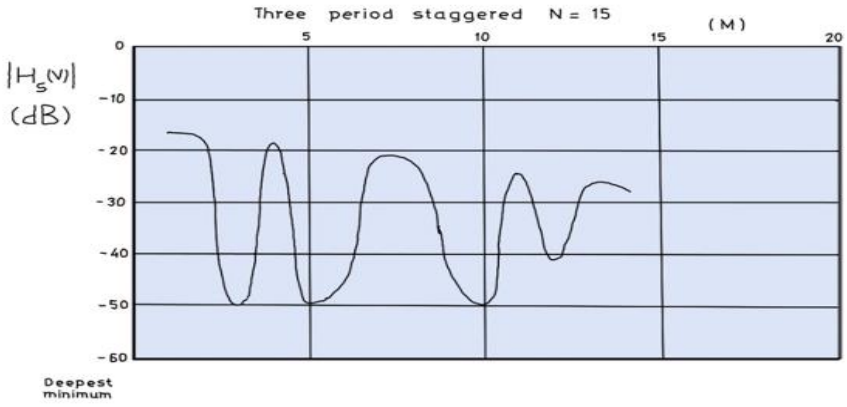

Figure 19: A Deepest Minimum in Response Curve Vs Stagger Delay (M)

ISSN 1533-9211

DOI: 10.5281/zenodo.8311139

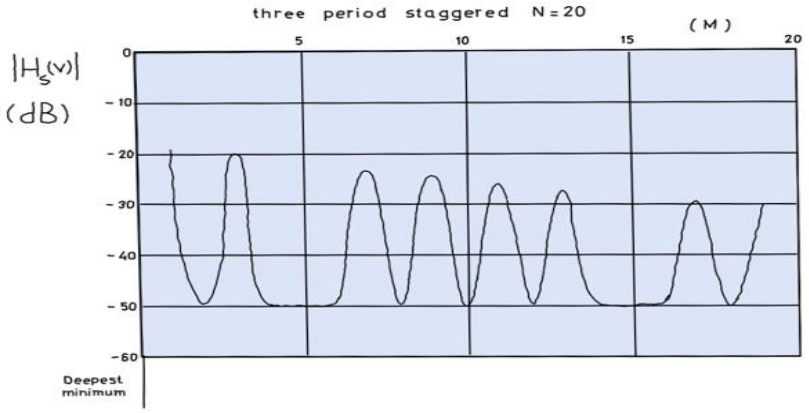

Figure 20: A Deepest Minimum in Response Curve Vs Stagger Delay (M)

Figure 21: A Deepest Minimum in Response Curve Vs Stagger Delay (M)

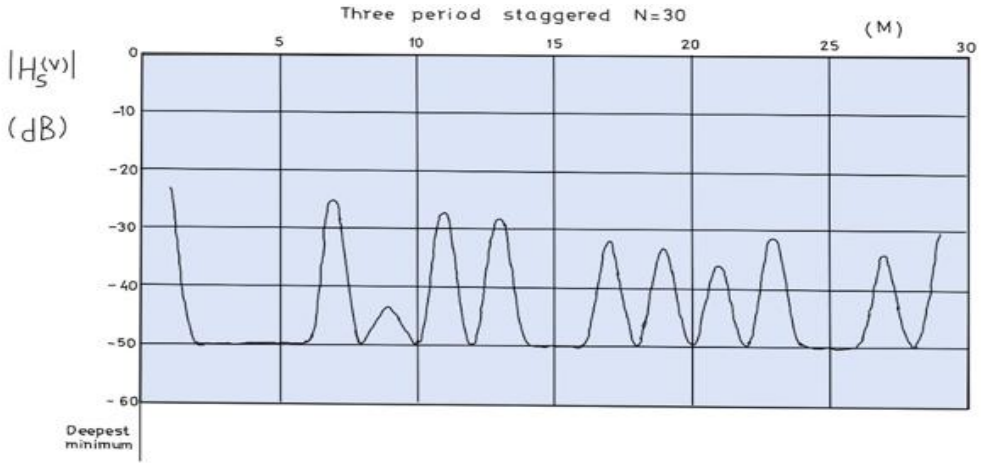

ISSN 1533-9211

DOI: 10.5281/zenodo.8311139

Figure 22: A Deepest Minimum in Response Curve Vs Stagger Delay (M)

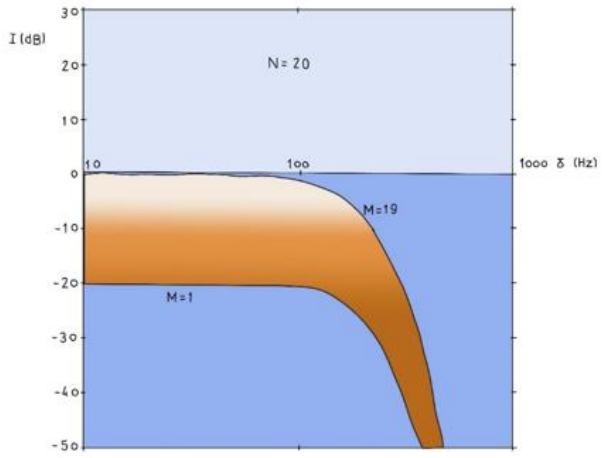

Figure 23: Improvement Factor for Three Period Stagger

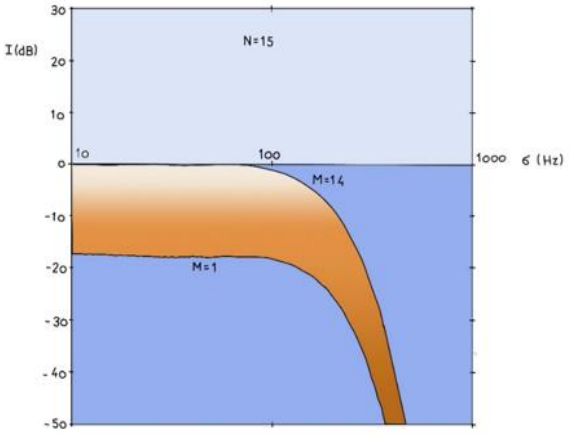

Figure 24: Improvement Factor for Three Period Stagger

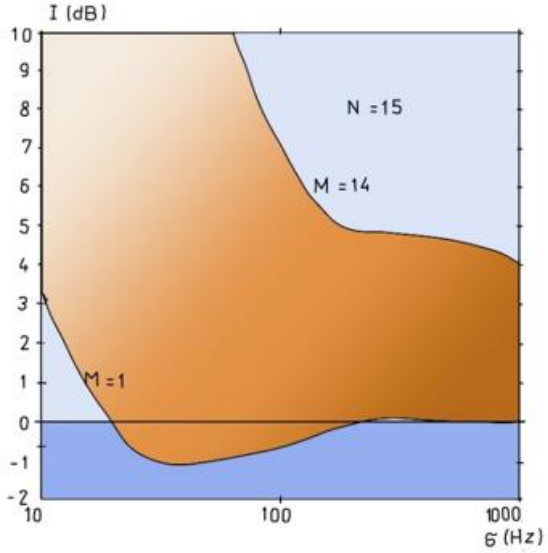

Figure 25: Improvement Factor for Tow-Period Stagger

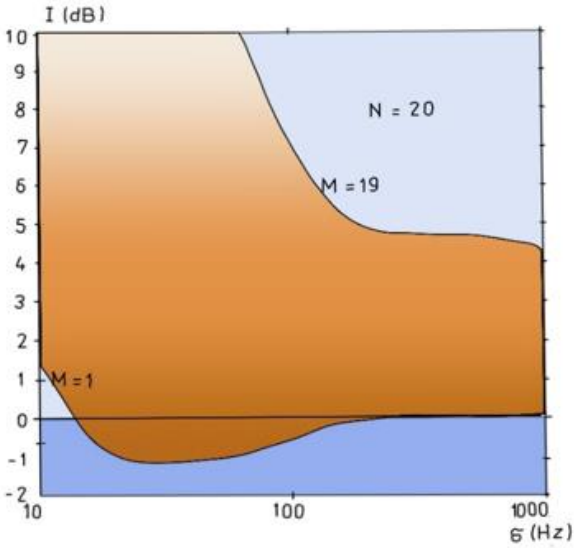

Figure 26: Improvement Factor for Three Period Stagger

ISSN 1533-9211

DOI: 10.5281/zenodo.8311139

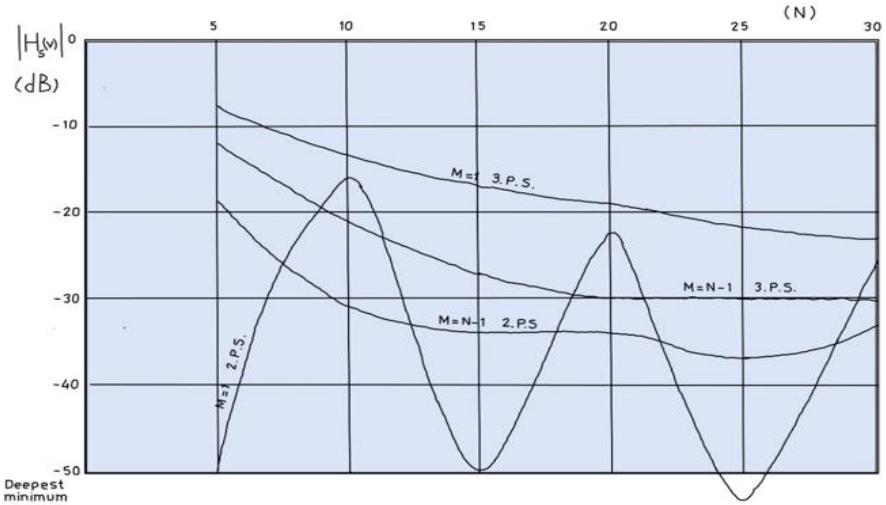

Figure 27: A Comparison between two and three Period Staggers at M=1, and M=N-1

References

1) Knott, Eugene F., John F. Schaeffer, and Michael T. Tulley. Radar cross section. SciTech Publishing, 2004.

2) Martone, Anthony F., Kenneth Ranney, and Calvin Le. "Noncoherent approach for through-the-wall moving target indication." IEEE Transactions on Aerospace and Electronic Systems 50.1 (2014): 193-206.

3) Zuyin, Weng. "Optimal design of clutter rejection filters for MTI system." 2001 CIE International Conference on Radar Proceedings (Cat No. 01TH8559). IEEE, 2001.

4) Martone, Anthony, Kenneth Ranney, and Roberto Innocenti. "Through-the-wall detection of slow-moving personnel." Radar Sensor Technology XIII. Vol. 7308. SPIE, 2009.

5) He, Qian, et al. "MIMO radar moving target detection in homogeneous clutter." IEEE Transactions on Aerospace and Electronic Systems 46.3 (2010): 1290-1301.

6) Zuyin, Weng. "Optimal design of clutter rejection filters for MTI system." 2001 CIE International Conference on Radar Proceedings (Cat No. 01TH8559). IEEE, 2001.

7) Bounaceur, Hamza, Ali Khenchaf, and Jean-Marc Le Caillec. "Analysis of small sea-surface targets detection performance according to airborne radar parameters in abnormal weather environments." Sensors 22.9 (2022): 3263.

8) Slob, Evert, Motoyuki Sato, and Gary Olhoeft. "Surface and borehole ground-penetrating-radar developments." Geophysics 75.5 (2010): 75A103-75A120.

9) Knott, Eugene F. Radar cross section measurements. Springer Science & Business Media, 2012.

10) Seltmann, Jörg EE. "Weather Radar." Springer Handbook of Atmospheric Measurements. Springer, Cham, 2021.841-900.

11) Martin, Jack. "High-volume manufacturing and field stability of MEMS products." Springer Handbook of Nanotechnology. Springer, Berlin, Heidelberg, 2010. 1803-1833.

12) Martin, Jack. "High-volume manufacturing and field stability of MEMS products." Springer Handbook of Nanotechnology. Springer, Berlin, Heidelberg, 2010. 1803-1833.

The Seybold Report
ISSN 1533-9211
DOI: 10.5281/zenodo.8311139

13) Dobkin, Bob, and Jim Williams, eds. "Analog circuit design: a tutorial guide to applications and solutions." (2011).

14) Astakhov, Viktor P. Geometry of single-point turning tools and drills: fundamentals and practical applications. Springer Science & Business Media, 2010.

15) Singh, Abhinav, VaibhaVshah, and Anurag Sarnaik. "Moving Target Indication Radar." International Journal of (2013).

16) Stanton, Timothy K., Wu-Jung Lee, and Kyungmin Baik. "Echo statistics associated with discrete scatterers: A tutorial on physics-based methods." The Journal of the Acoustical Society of America 144.6 (2018): 3124-3171.

17) Zia, Roseanna N. Individual particle motion in colloids: Microviscosity, microdiffusivity, and normal stresses. California Institute of Technology, 2011.

18) Scherer, Sebastian, Lyle Chamberlain, and SanjiVsingh. "Autonomous landing at unprepared sites by a full-scale helicopter." Robotics and Autonomous Systems 60.12 (2012): 1545-1562.

19) Fulton, Caleb, et al. "Cylindrical polarimetric phased array radar: Beamforming and calibration for weather applications." IEEE Transactions on Geoscience and Remote Sensing 55.5 (2017): 2827-2841.

20) Atzeni, C., et al. "Early warning monitoring of natural and engineered slopes with ground-based synthetic-aperture radar." Rock Mechanics and Rock Engineering 48.1 (2015): 235-246.

21) Kavitha, L. Babu Saraswathi, and I. Jacob Raglend. "A wide-scan phased array antenna for a small active electronically scanned array: a review." 2013 International Conference on Circuits, Power and Computing Technologies (ICCPCT). IEEE, 2013.

22) Schvartzman, David, Sebastián M. Torres, and Tian-You Yu. "Motion-compensated steering: Enhanced azimuthal resolution for polarimetric rotating phased array radar." IEEE Transactions on Geoscience and Remote Sensing 59.12 (2021): 10073-10093.

23) Weierstall, Uwe, J. C. H. Spence, and R. B. Doak. "Injector for scattering measurements on fully solvated biospecies." Review of Scientific Instruments 83.3 (2012): 035108.

24) Mounaix, Mickael, et al. "Spatiotemporal coherent control of light through a multiple scattering medium with the multispectral transmission matrix." Physical review letters 116.25 (2016): 253901.

25) Swindlehurst, A. Lee, et al. "Applications of array signal processing." Academic Press Library in Signal Processing. Vol. 3. Elsevier, 2014. 859-953.

26) Fox, Zachary W., et al. "Implementation of continuous fast scanning detection in femtosecond Fourier-transform two-dimensional vibrational-electronic spectroscopy to decrease data acquisition time." Review of Scientific Instruments 89.11 (2018): 113104.

27) Cui, Kaihua, et al. "Scanning error detection and compensation algorithm for white-light interferometry." Optics and Lasers in Engineering 148 (2022): 106768.

28) Cui, Kaihua, et al. "Scanning error detection and compensation algorithm for white-light interferometry." Optics and Lasers in Engineering 148 (2022): 106768.

29) Chen, Xiaolong, et al. "Detection and extraction of target with micromotion in spiky sea clutter via short-time fractional Fourier transform." IEEE Transactions on Geoscience and Remote Sensing 52.2 (2013): 1002-1018.

30) Narbudowicz, Adam, Max J. Ammann, and Dirk Heberling. "Switchless reconfigurable antenna with 360° steering." IEEE Antennas and Wireless Propagation Letters 15 (2016): 1689-1692.